BASED ON PT-FUNCTIONALIZED HIERARCHICAL ZNO MICROSPHERES, THE TRIETHYLAMINE GAS SENSOR

K C Kavitha[1*], A.Rathinam[2],S.Rathinavel[3],

[1]Department of Electrical and Electronics Engineering,Bharathiyar Instute of Engineering for Women, salem Tamilnadu 636112.
[2,3]Department of Electrical and Electronics Engineering, Paavai Engineering College (Autonomous),Namakkal, Tamilnadu 637018.

A B S T R A C T

Triethylamine (TEA) gas monitoring and detection are essential for ensuring both environmental and human safety. The TEA gas sensor, however, has a poor response rate. Unique nanosized-Pt-decorated hierarchical ZnO is presented here. There were made microspheres. Compared to pure ZnO microspheres and Pt-c-ZnO (deposited Pt nanoparticles), the resultant Pt-ZnO displayed the best TEA gas sensing characteristics, in terms of decreased detection limits on commercial ZnO). Greater selectivity, a higher operating temperature (200 C), and long-term stability. Notably, Pt-reaction ZnO's value in the direction of 100 ppm TEA was as high as 242, 50 and 16 times higher than those of clean ZnO and Ptc- respectively, a ZnO sensor. In addition to structural advantages, the superior attributes were attributed to ZnO and Pt work together in harmony. The electron-sinker effect of Pt provided a full explanation of the sensing mechanism. Density function theory (DFT) simulation and the Kelvin probe provided more confirmation. Furthermore, temperature programmed desorption (O2-TPD) and DFT simulation showed that this ideal sample had higher surface oxygen activity and decreased TEA adsorption energy. Pt-ZnO is a good contender for TEA gas sensors based on the aforementioned benefits. This work is significant because it creates a new perspective on how performance enhancement works.

Keywords: Pt-ZnO microspheres Triethylamine sensor High response Gas sensing mechanism

1. Introduction

Triethylamine (TEA), a colourless, transparent liquid with a potent ammonia-like odour, has been utilised as raw materials, catalysts, and solvents. Materials used in the field of organic synthesis [1,2]. Additionally, numerous According to studies, TEA is released by deceased fish and other marine life. and over time, its concentration progressively rises [3,4]. Consequently, to evaluate the calibre of marine food, TEA can be employed as a chemical tracer. Life. However, it has a major negative impact on human health. After a large exposure, headache issues, gastroenteritis, and pulmonary Death and edoema both happen [5, 6]. Additionally, verifiable evidence implies that by combining with air, it can endanger our ecosystem, which, when exposed to fire sources, even explodes. Consequently, it's to use techniques with high sensitivity and selectivity to monitor TEA. Numerous spectroscopic tools have currently been used effectively in the very accurate detection of TEA.

However, their limited application is due to their cumbersome and uncomfortable operations. Fortunately, metal oxide semiconductors like ZnO [7], SnO_2 [8], Fe_2O_3 [9], In2O_3 [10], and WO_3 [11] are attractive candidates for TEA gas sensors due to their fascinating qualities, which include ease of fabrication, affordability, and outstanding stability. Due to their adjustable shape, quick electron mobility, strong chemical stability, and low production cost, TEA gas sensors based on ZnO are the most well-liked among them [12–14]. However, because to their high working temperature, low sensitivity, and poor selectivity, they have limited practical applicability. Liu et al. decreased the operating temperature of a TEA gas sensor based on Zn_2SnO_4-ZnO to 198 C to address these problems, however their sensor's response ranged only from 176 to 100 ppm TEA [15]. Wei et al. recently published a paper on a TEA gas sensor based on ZnO species with various donor defect ratios and a low detection limit. Its operating temperature, however, is up to 276 °C [16]. Melioration is therefore required to get past these flaws. Manipulating morphology is one strategy.

Numerous morphologies have been used, including nanoparticles, nanowires, nanorods, and nanoflowers. The influence of morphology on detecting qualities is evident, just like with other metal oxide-based sensors [17,18]. ZnO gas sensors with 3D structures (hierarchical microspheres) have shown improved performance compared to 1D (or 2D) nano-materials (nanoparticles [18], nanowires [19], and nanorods [20]). They have a larger effective specific surface area than their 1D/2D counterparts, which explains this. Additionally, the high detect limit, poor selectivity, and lengthy response and recovery times of gas sensors based on unitary metal oxides have their drawbacks [22–24]. As a result, ZnO that is operated by noble metals is a sensible choice. According to literature findings, the decorating of noble metal particles could further improve gas sensing skills. For instance, Katoch et al. showed that Pt nanoparticle-decorated ZnO nanowire sensors were capable of detecting benzene at room temperature, and that their overall performance was superior to that of virgin ZnO nanowires [25]. According to Song et al., Au nanoparticle-modified ZnO sensors had an extremely high response value of 22-100 ppm TEA, which was superior to pure ZnO sensors.

Following the aforementioned outline, we used a simple hydrothermal approach to create unique hierarchical ZnO microspheres made of porous nanosheets. Afterward, we added Pt nanoparticles. It. In contrast, pristine ZnO and commercial ZnO both worked with Pt. Additionally, microspheres were employed as control specimens. The gas sensing capabilities these three samples underwent examination. The result indicate that the Pt-ZnO microsphere-based TEA gas sensor has superior performance. More sensitive and more selective than the other two samples. Additionally, the gas this article discusses a sensing mechanism improved by Pt-ZnO microspheres. Based on the suitable energy band topologies, in great detail.

2. Experimental

2.1. Materials

Shanghai Chemical Industrial Company provided all of the reagents. The analytical-grade chemicals included zinc acetate $[Zn(Ac)_2]2H_2O$, trisodium citrate $[Na_3C_6H_5O_7]2H_2O$, urea $[CO(NH_2)_2]$, chloroplatinic acid $[H_2PtCl_6]$, and sodium borohydride, all of which could be used for experiments without further purification ($NaBH_4$).

2.2. Synthesis

2.2.1. Preparation of ZnO microspheres

We created hierarchical ZnO microspheres in accordance with our prior report [27,28]. Typically, 79 mL of water was used to dissolve 0.67 g of $Zn(Ac)_2$ in, 0.37 g of $CO(NH_2)_2$, and 0.07 g of $Na_3C_6H_5O_7$ in. distilled water. The mixture was continuously stirred for approximately 30 minutes. The following phase involved hydrothermal treatment for 6 hours at 121 C. The centrifugation technique was used to collect the precipitate. is zinc By drying at 80°C for the entire night, hydroxide carbonate was obtained. The hierarchical ZnO microspheres were then created using the At 300 °C for two hours, zinc hydroxide carbonate was calcined in the air.

2.2.2. Function of Pt nanoparticles

0.06 g of ZnO microspheres were dissolved in deionized water using an ultrasonic system, and then 1 mL of $H_2PtCl_66H_2O$ (2.55 mmol L 1) was added while being vigorously stirred. To the aforementioned mixture, 1 mL of deionized water containing 0.4 mg of NaBH4 was then added drop by drop. About two hours were spent stirring the mixture, followed by washing it with deionized water and 100% ethanol before centrifuging it. The particles were identified as Pt-ZnO microspheres after being dried at 65 °C overnight. Inductively coupled plasma mass spectrometry was used to determine the actual ratio of Pt in the composite, which was 0.85 weight percent (ICPMS). The same method was used to create Pt-c-ZnO, however instead of using ZnO microspheres, commercial ZnO was used instead.

2.3. Characterization

These three materials' crystal structures were discovered using X-ray diffraction (XRD-6100, =0.15 nm, Shimadzu, Japan). Transmission electron microscopy (TEM) and field-emission scanning electron microscopy (FE-SEM, JSM-7490 F, JEOL, and Japan) were used to get the nanostructures of the items as obtained (JEOL JEM-2100 F). In order to determine the Brunauer-Emmett-Teller (BET) surface area (S_{BET}) of the samples, N2 adsorption data were collected using a Micrometrics TriStar II 3021 device (USA). Using desorption data, the pore size distributions were assessed using the Barret-Joyner-

Halender (BJH) method. X-ray photoelectron spectroscopy was used to determine each element's chemical state (XPS, Thermo ESCALA 251). On a BELCAT-B equipment, the temperature programmed desorption (O2-TPD) tests were examined (Japan).

2.4. Gas sensing measurement

An earlier technique [29–32] was used to evaluate the effectiveness of gas sensors based on the as-synthesised samples. The image of a typical sensor is depicted in Fig. 1, and its design was carried out as follows: First, the finished goods were ground into a paste in an agate mortar after being dissolved in 0.5 mL of deionized water. The surface of an alumina ceramic tube measuring 4 mm in length and 1 mm in diameter was then painted uniformly with it. It was important to note that the tube had two gold electrode rings designed at either end, allowing for the recording of the constructed sensor's resistance. The gold electrodes should therefore be completely covered. Four Pt wires were additionally attached to the gold electrodes on one end to ensure the collection of resistance signals and to the test panel on the other end to orient the tube. The operating temperature could be changed by adjusting the heating voltage using a Ni-Cr coil that was put into the tube to act as a heater. Side-heated gas sensors were created after being air dried and aged for two days. The gas sensors were then placed in the test chamber of the WS-30A measuring system (Winsen Electronics Co. Ltd., Zhengzhou, China). The computer displays the online register of voltage change across the reference resistor. The sensors' reaction can then be computed appropriately [32]. S = Ra/Rg, where Ra is the resistance in ambient air and Rg is the resistance in a mixture of the tested gas and air, is the definition of the sensor response. In the case of adsorption and desorption, respectively, the response and recovery periods are defined as the times at which the sensor attained 90% of the total resistance change.

3. Results and discussion

3.1. Structural, morphological and compositional results

The XRD patterns for ZnO, Pt-c-ZnO, and Pt-ZnO microspheres are displayed in Fig. 1. It has been noted that all three of these samples' diffraction peaks are precisely indexed to hexagonal wurtzite-structured ZnO (JCPDS Card No. 65-3411) [33]. However, there are no typical peaks that are connected to Pt, which is possibly because there is so little Pt [34]. XPS measurements were performed to validate the existence of Pt and the direction in which electrons flow across the interface between ZnO and Pt. The results are displayed in Fig. 2. For ZnO and Pt-ZnO, the survey spectra in Fig. 2a show the presence of Zn and O components, and the signal attributed to Pt is undetectable in the latter. The distinctive peaks of Pt 4f7/2 and 4f5/2 are evident in the high resolution XPS spectrum of Pt-ZnO. (Fig. 2b). The valence state of Pt particles in Pt-ZnO is also zero, with the exception of a negative shift (0.2 eV) when compared to the XPS spectrum of Pt with high purity [35]. Zn 2p3/2, Zn 2p1/2, and O 1s distinctive peaks can be distinguished inFig. 3c and d, respectively [36]. In comparison to ZnO microspheres, the

typical binding energies of Zn 2p3/2, Zn 2p1/2, and O 1s in Pt-ZnO microspheres exhibit a modest positive shift. Overall, based on the variations in the binding energies, we deduce that when two pieces of ZnO or Pt come into contact, electrons move from one to the other [37,38].

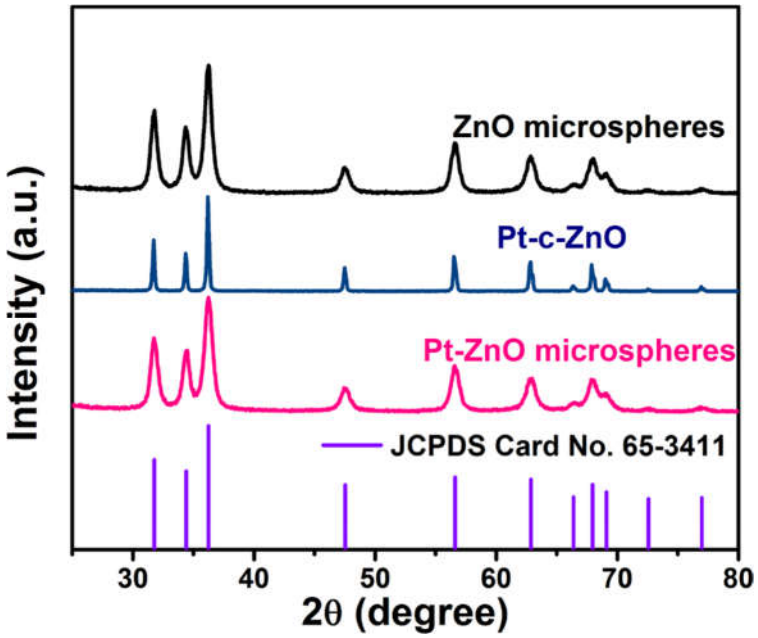

Fig. 1. XRD patterns for the pristine ZnO microspheres, Pt-c-ZnO and the Pt- ZnO microspheres.

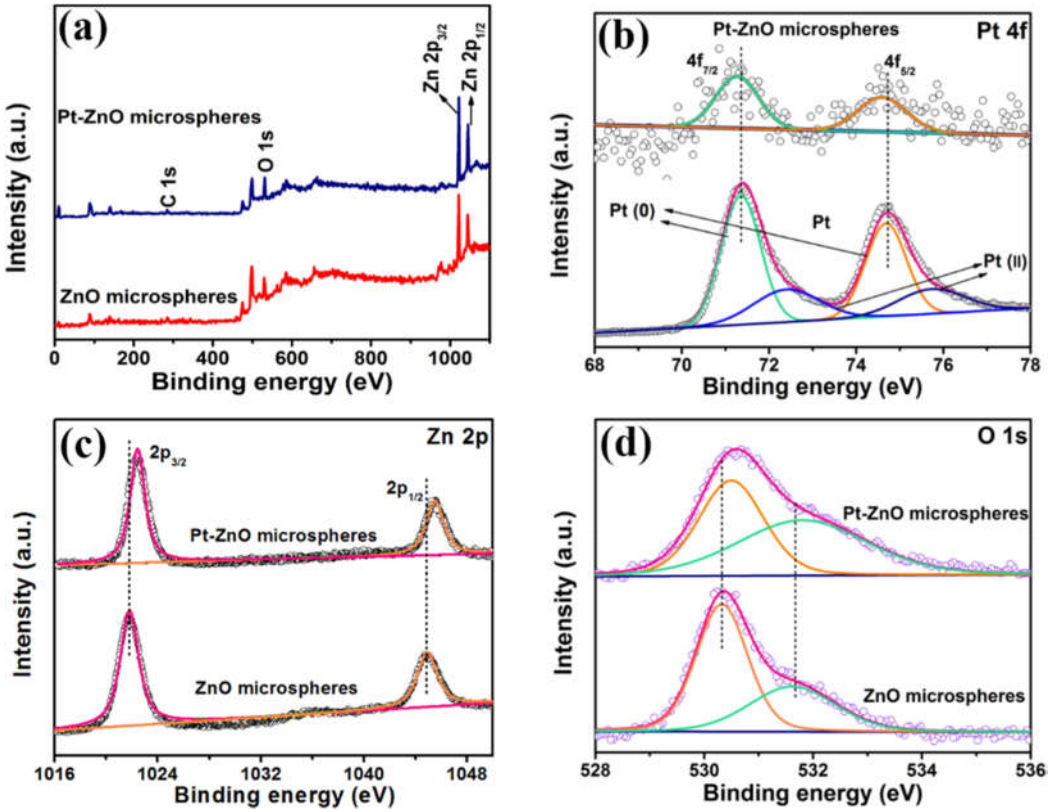

Fig. 2. (a) XPS survey spectra of Pt-ZnO microspheres, (b-d) High-resolution XPS spectra of Pt 4f, Zn 2p, and O 1s, respectively.

SEM and TEM observations were carried out to investigate the sample morphologies. The SEM images of ZnO and Pt-ZnO microspheres, respectively, are shown in Figures. It is obvious that this microsphere's edge is translucent and thin. And this microsphere's centre is black with few brilliant spots, indicating that big pores have formed as a result of the presence of CO(NH2)2. The hierarchical architectures of the ZnO microspheres are likewise confirmed by this. Reasonably, the TEM photos show discrete Pt nanoparticles. The interplanar spacing distance of 2.27 Å measured in Fig. 2d corresponds to the (111) plane of cubic phase Pt [39]. And the interplanar spacing distances of 2.62 Å and 2.80 Å fit well with the (002) and (100) planes of wurtzite phase ZnO, respectively [40].

4. Conclusions

In conclusion, Pt-ZnO microspheres enable the development of an excellently performing TEA gas sensor. A straightforward and environmentally friendly technology is successful in creating the hierarchically structured microspheres. Pt-ZnO microsphere sensors are superior to ZnO microsphere sensors and Pt-c-ZnO sensors for gas sensing. Compared to its competitors, this appealing sensor responds to 100 ppm of TEA with a response of around 243. Additionally, this sensor exhibits excellent stability and good TEA selectivity. The catalytic and electron-sinking effects of Pt, high active oxygen species and low TEA adsorption, as well as the distinctive shapes, can be credited for the improvement of Pt-ZnO microspheres as TEA sensors. Based on the aforementioned findings and discussion, Pt-ZnO microspheres show promise as TEA gas sensors.

References

[1] Y.Z. Lv, C.R. Li, G. Lin, F.C. Wang, X. Yue, X.F. Chu, Triethylamine gas sensor based on ZnO nanorods prepared by a simple solution route, Sens. Actuators B Chem. 141 (2009) 85–88.

[2] H. Xu, J. Ju, W. Li, J. Zhang, J. Wang, B. Cao, Superior triethylamine-sensing properties based on TiO2 /SnO2 n–n heterojunction nanosheets directly grown on ceramic tubes, Sens. Actuators B Chem. 228 (2016) 634–642.

[3] E.X. Chen, H.R. Fu, R. Liu, Y.X. Tan, Highly selective and sensitive trimethylamine gas sensor based on cobalt imidazolate framework material, ACS Appl. Mater. Interfaces 6 (2014) 22871–22875.

[4] K. Mitsubayashi, Y. Kubotera, K. Yano, Y. Hashimoto, T. Kon, Trimethylamine biosensor with flavin-containing monooxygenase type 3 (FMO3) for fish-freshness analysis, Sens. Actuators B Chem. 103 (2004) 463–467.

[5] H.S. Woo, W.N. Chan, I.D. Kim, J.H. Lee, Highly sensitive and selective trimethylamine sensor using one-dimensional ZnO-Cr2O3 hetero-nanostructures, Nanotechnology 23 (2012), 245501.

[6] D.X. Ju, H.Y. Xu, Z.W. Qiu, Z.C. Zhang, Q. Xu, J. Zhang, J.Q. Wang, B.Q. Cao, Near room temperature, fast-response, and highly sensitive triethylamine sensor assembled with Au-loaded ZnO/SnO2 core-shell nanorods on flat alumina substrates, ACS Appl. Mater. Interfaces 7 (2015) 19163–19171.

[7] Y. Li, Z. Tao, N. Luo, G. Sun, B. Zhang, H. Jin, H. Bala, J. Cao, Z. Zhang, Y. Wang, Single-crystalline porous nanoplates-assembled ZnO hierarchical microstructure with superior TEA sensing properties, Sens. Actuators B Chem. 290 (2019) 607–615.

[8] Y. Xu, L. Zheng, C. Yang, W. Zheng, X. Liu, J. Zhang, Oxygen vacancies enabled porous SnO2 thin films for highly sensitive detection of triethylamine at room temperature, ACS Appl. Mater. Interfaces 12 (2020) 20704–20713.

[9] X. Song, Q. Xu, T. Zhang, B. Song, C. Li, B. Cao, Room-temperature, high selectivity and low-ppm-level triethylamine sensor assembled with Au decahedrons-decorated porous α-Fe2O3 nanorods directly grown on flat substrate, Sens. Actuators B Chem. 268 (2018) 170–181.

[10] L. Zheng, T. Ma, Y. Zhao, Y. Xu, L. Sun, J. Zhang, X. Liu, Synergy between Au and In2O3 microspheres: a superior hybrid structure for the selective and sensitive detection of triethylamine, Sens. Actuators B Chem. 290 (2019) 155–162.

[11] Y. Han, Y. Liu, C. Su, X. Chen, M. Zeng, N. Hu, Y. Su, Z. Zhou, H. Wei, Z. Yang, Sonochemical synthesis of hierarchical WO3 flower-like spheres for highly efficient triethylamine detection, Sens. Actuators B Chem. 306 (2020), 127536.

[12] I.S. Hwang, S.J. Kim, J.K. Choi, J. Choi, H. Ji, G.T. Kim, G. Cao, J.H. Lee, Synthesis and gas sensing characteristics of highly crystalline ZnO–SnO2 core–shell nanowires, Sens. Actuators B Chem. 148 (2010) 595–600.

[13] K.W. Kim, P.S. Cho, S.J. Kim, J.H. Lee, C.Y. Kang, The selective detection of C2H5OH using SnO2-ZnO thin film gas sensors prepared by combinatorial solution deposition, Sens. Actuators B Chem. 123 (2007) 318–324.

[14] Z. Qin, Y.H. Huang, J.J. Qi, H.F. Li, J. Su, Y. Zhang, Facile synthesis and photoelectrochemical performance of the bush-like ZnO nanosheets film, Solid State Sci. 14 (2012) 155–158.

[15] F. Liu, X. Chen, X. Wang, Y. Han, X. Song, J. Tian, X. He, H. Cui, Fabrication of 1D Zn2SnO4 nanowire and 2D ZnO nanosheet hybrid hierarchical structures for use in triethylamine gas sensors, Sens. Actuators B Chem. 291 (2019) 155–163.

[16] W. Wei, J. Zhao, S. Shi, H. Lin, Z. Mao, F. Zhang, F. Qu, Boosting ppb-level triethylamine sensing of ZnO: adjusting proportions of electron donor defects, J. Mater. Chem. C 8 (2020) 6734–6742.

[17] K. Shingange, Z.P. Tshabalala, O.M. Ntwaeaborwa, D.E. Motaung, G.H. Mhlongo, Highly selective NH3 gas sensor based on Au loaded ZnO nanostructures prepared using microwave-assisted method, J. Colloid Interface Sci. 479 (2016) 127–138.

[18] A.A. Ismail, F.A. Harraz, M. Faisal, A.M. El-Toni, A. Al-Hajry, M.S. Al-Assiri, A sensitive and selective amperometric hydrazine sensor based on mesoporous Au/ ZnO nanocomposites, Mater. Design 109 (2016) 530–538.

[19] Z. Yuan, Y. Lei, H. Ding, W. Huang, C. Shuai, J. Deng, One-step synthesis of single-crystalline ZnO nanowires for the application of gas sensor, J. Mater. Sci.-Mater. El. 29 (2018) 11559–11565.

[20] N.J. Ridha, F.K. Alosfur, H.J.M. Hafizuddin, R. Shahidan, Dimensional effect of ZnO nanorods on gas sensing performance, J. Phys. D Appl. Phys. 51 (2018), 435101.

[21] W. Li, H. Xu, H. Yu, T. Zhai, X. Qi, X. Yang, J. Wang, B. Cao, Different morphologies of ZnO and their triethylamine sensing properties, J. Alloys. Compd. 706 (2017) 461–469. [22] Z. Lou, F. Li, J. Deng, L. Wang, T. Zhang, Branch-like hierarchical heterostructure (α-Fe2O3/TiO2): a novel sensing material for trimethylamine gas sensor, ACS Appl. Mater. Interfaces 5 (2013) 12310–12316.

[23] J. Liu, M. Dai, T. Wang, P. Sun, X. Liang, G. Lu, K. Shimanoe, N. Yamazoe, Enhanced gas sensing properties of SnO2 hollow spheres decorated with CeO2 nano-particles heterostructure composite materials, ACS Appl. Mater. Interfaces 8 (2016) 6669–6677. [24] C. Wang, X. Cui, J. Liu, X. Zhou, X. Cheng, P. Sun, X. Hu, X. Li, J. Zheng, G. Lu, Design of superior ethanol gas sensor based on Al-doped NiO nanorod-flowers, ACS Sens. 1 (2016) 131–136.

[25] A. Katoch, S.W. Choi, G.J. Sun, S.S. Kim, Pt nanoparticle-decorated ZnO nanowire sensors for detecting benzene at room temperature, J. Nanosci. Nanotechnol. 13 (2013) 7097–7099.

[26] X. Song, Q. Xu, H. Xu, B. Cao, Highly sensitive gold-decorated zinc oxide nanorods sensor for triethylamine working at near room temperature, J. Colloid Interface Sci. 499 (2017) 67–75.

[27] C. Lei, M. Pi, C. Jiang, B. Cheng, J. Yu, Synthesis of hierarchical porous zinc oxide (ZnO) microspheres with highly efficient adsorption of Congo red, J. Colloid Interface Sci. 490 (2017) 242–251.

[28] S. Wang, P. Kuang, B. Cheng, J. Yu, C. Jiang, ZnO hierarchical microsphere for enhanced photocatalytic activity, J. Alloys. Compd. 741 (2018) 622–632.

[29] F. Gu, H. Chen, D. Han, Z. Wang, Metal-organic framework derived Au@ZnO yolk-shell nanostructures and their highly sensitive detection of acetone, RSC Adv. 6 (2016) 29727–29733.

[30] A. Abdurahman, P. Nizamidin, A. Yimit, Optical and electrochemical gas sensing properties of yttrium–silver co-doped lithium iron phosphate thin films, Mater. Sci. Semicond. Process. 22 (2014) 21–27.

[31] F. Tian, Y. Liu, K. Guo, Au nanoparticle modified flower-like ZnO structures with their enhanced properties for gas sensing, Mater. Sci. Semicond. Process. 21 (2014) 140–145.

[32] H. Zhang, P. Song, D. Han, H. Yan, Z. Yang, Q. Wang, Controllable synthesis of novel ZnSn(OH)6 hollow polyhedral structures with superior ethanol gas-sensing performance, Sens. Actuators B Chem. 209 (2015) 384–390.

[33] Y. Zhu, D. Liu, Y. Lai, M. Ming, Ambient ultrasonic-assisted synthesis, stepwise growth mechanisms, and photocatalytic activity of flower-like nanostructured ZnO and Ag/ZnO, J. Nanopart. Res. 16 (2014) 1–13.

[34] J. Ye, B. Cheng, S. Wageh, A.A. Al-Ghamdi, J. Yu, Flexible Mg-Al layered double hydroxide supported Pt on Al foil for use in room-temperature catalytic decomposition of formaldehyde, RSC Adv. 6 (2016) 34280–34287.

[35] L. Pino, A. Vita, M. Cordaro, V. Recupero, M.S. Hegde, A comparative study of Pt/ CeO2 catalysts for catalytic partial oxidation of methane to syngas for application in fuel cell electric vehicles, Appl. Catal. A-Gen. 243 (2003) 135–146.

[36] N. Nie, F. He, L. Zhang, B. Cheng, Direct Z-scheme PDA-modified ZnO hierarchical microspheres with enhanced photocatalytic CO2 reduction performance, Appl. Surf. Sci. 457 (2018) 1096–1102. [37] Q. Xu, L. Zhang, J. Yu, S. Wageh, A.A. Al-Ghamdi, M. Jaroniec, Direct Z-scheme photocatalysts: principles, synthesis, and applications, Mater. Today 21 (2018) 1042–1063.

[38] J. Low, B. Dai, T. Tong, C. Jiang, J. Yu, In situ irradiated X-Ray photoelectron spectroscopy investigation on a direct Z-Scheme TiO2/CdS composite film photocatalyst, Adv. Mater. 31 (2019), 1802981.

[39] Z. Zhu, S.H. Huang, C.X. Liu, R.J. Wu, Fabrication of Pd-Pt/ZnO for high sensitive gaseous formaldehyde sensor, J. Nanosci. Nanotechno. 18 (2018) 1682–1687.

[40] X. Ke, G. Zhu, D. Yong, Y. Shen, J. Yang, J. Liu, Fabrication of Pt-ZnO composite nanotube modified electrodes for the detection of H2O2, J. Electroanal. Chem. 817 (2018) 176–183.